SCIENCE CHINA
Information Sciences

• RESEARCH PAPER •

October 2021, Vol. 64 202204:1–202204:15
https://doi.org/10.1007/s11432-020-3072-9

Distributed H_∞ filtering of nonlinear systems with random topology by an event-triggered protocol

Yun CHEN[1], Mengze ZHU[1], Renquan LU[2*] & Anke XUE[1]

[1]*Key Lab for IoT and Information Fusion Technology of Zhejiang, Hangzhou Dianzi University, Hangzhou* 310018*, China;*
[2]*School of Automation, Guangdong University of Technology, Guangzhou* 510006*, China*

Received 10 May 2020/Revised 2 July 2020/Accepted 1 September 2020/Published online 15 September 2021

Abstract Applying an event-triggered protocol, this paper proposes a distributed H_∞ filter design for nonlinear perturbed systems under fading measurements with random topology. Nonlinearities in this system obey the one-sided Lipschitz constraint, which embraces the conventional Lipschitz condition as a special case. The sensor network allows random variations of the interconnection strengths between adjacent nodes, and the connection coefficient is determined as the product of a constant and a stochastic variable with a known probabilistic feature. To reduce the unnecessary data transmission and efficiently use the limited bandwidth, the transmissions are orchestrated by an event-triggered regulating strategy. A stochastic bounded real lemma is established for the resulting error dynamics. Based on the presented matrix decomposition, which removes the direct coupling between the statistical information of interconnection strengths and the filter gain, the distributed H_∞ filter gain can be explicitly expressed and easily solved. The usefulness of the theoretical method is demonstrated in a simulation study.

Keywords sensor network, distributed H_∞ filtering, one-sided Lipschitz condition, event-triggered protocol, random topology

Citation Chen Y, Zhu M Z, Lu R Q, et al. Distributed H_∞ filtering of nonlinear systems with random topology by an event-triggered protocol. Sci China Inf Sci, 2021, 64(10): 202204, https://doi.org/10.1007/s11432-020-3072-9

1 Introduction

A sensor network is a complicated networked system of many sensor nodes that perform sensing/measuring, data processing, and communication. A wireless sensor network is a cutting-edge technology with distinctive features including low cost, high scalability, and self-organization. Owing to these advantages, wireless sensor networks have been deployed in surroundings monitoring, battle-field surveillance, industrial and agricultural productions, and various other applications [1–3]. A distributed filtering/estimation framework in a sensor network has specific spatial characteristics that are preferred over the centralized scheme, because the distributed strategy can use the information from a given sensor node and its adjacent nodes in the estimation/filtering task [4]. In recent years, solutions to estimation/filtering design problems over sensor networks have attracted much interest [4–10].

In practical applications, information is distributed over a public communication channel with limited bandwidth, causing undesirable networked-induced phenomena such as data losses and disorders, transmission delays, and non-ideal measurements. As these anomalies inevitably lead to performance degradation [4, 11, 12], many researchers have investigated distributed estimation/filtering in networks flawed by these unfavorable effects. Liang et al. [13] considered the distributed estimation problem in systems subjected to randomly occurring nonlinear uncertainties and missing measurements. They modeled the distribution of missing measurements by a Bernoulli-type stochastic variable, and designed the corresponding filter by assessing the feasibilities of convex optimization problems. Similarly to [13], Wang et al. [14] investigated the distributed filtering of positive systems with Bernoulli-distributed imperfect measurements and sector-bounded nonlinear uncertainties. The distributed filtering and estimation

* Corresponding author (email: rqlu@gdut.edu.cn)

problems for systems with fading measurements described by stochastic sequences with known statistical information were studied in [5, 15, 16].

The unsatisfactory phenomena in network settings are primarily caused by the contradictory needs to increase the data-transmission volume and cut down the communication bandwidth occupancy. When the communication constraints are specified in advance, this dilemma is efficiently solved by reducing the transmission quantities or frequencies, which notably reduces the occupancy rates of the communication resources. Data transmissions are commonly regulated by time-triggered communication protocols [17–22] and event-triggered transmission policies [4, 9, 23–26]. In communication protocols based on time triggering, only the 'selected' data (a subset of all data) will be admitted to the communication channel at each instant. In contrast, event-triggered-based policies do not require data transmission at each instant. An event-triggered scheduling framework permits signal transmission only when the variations in measurement data are sufficiently large, or data transmissions at other instants without notable changes are forbidden. In this framework, the communication resources are not always occupied and are available for other network users [4,23,27,28]. The event-triggered scheduling strategy can efficiently operate under the communication constraints of large scale spatially distributed systems [4, 9, 29–32].

The systems in practical applications are frequently perturbed by nonlinearities, which degrade the dynamic performance and probably also lead to instability. In the existing literature, nonlinearly perturbed functions are usually constrained by the standard Lipschitz conditions, which are easily expressed as certain quadratic constrained forms [33–35]. Unlike the normal Lipschitz restriction satisfying the so-called two-sided inequality, the one-sided Lipschitz condition does not require a positive Lipschitz constant. Consequently, the one-sided Lipschitz type nonlinearity constraint is more general than the classical Lipschitz restriction [34]. The adaptive distributed consensus control problem has been considered for one-sided Lipschitz nonlinear multi-agents systems with unknown communication topologies [36]. However, event-triggered protocol-based distributed filtering in a sensor network setting under undesired measurements has never been treated for a one-sided Lipschitz type system. This lack of theoretical and applied knowledge was the first motivator of our present research.

The property of a large-scale spatially networked system largely relies on the topological structure of the system, including the connectivity and connection strengths among the individual nodes. The topological structure of an ideal sensor network is assumed to be known and time-invariant, but the structure of a realistically distributed model is characterized by uncertainty and/or randomness among the individuals in the network, and is not time-invariant. Uncertainty and stochasticity in the topology of a spatially distributed system are mainly (but not solely) caused by connection failures in hostile surroundings and adversarial attacks, changes in relative positions due to individual movements, and variations in the surroundings (such as humidity, temperature, quality of the communication environment, and transient appearances/disappearances of obstacles among the individuals). Clearly, the interconnection strengths must be acquired by statistical approaches and measurement technologies [4,37,38]. A typical example is a wireless sensor network with random topology caused by a false data-injection attack [37]. The random topology of multi-agent systems governed by a Markov chain has also been investigated [39]. Several researchers [40–42] have considered distributed filtering/estimation in a Markov switching topology, and have solved network problems by Markov jumping system theory. An example is the distributed filter design method of Liu et al. [43], which is based on an event-triggered transmission scheme in a Markov switching topology. Topology switching has been implemented by a semi-Markovian chain [44] and a predetermined switching rule [45]. A network topology can be represented not only as a Markov chain, but also as a Bernoulli sequence that captures the random switching in the topological structure of a class of complex stochastic networks [46].

The Bernoulli-type binary distribution in [46] describes the random connectivity between any two nodes, but cannot quantify the incremental or decremental characteristics of the interconnection coefficients. In contrast, the Markov chain-based switching topology reflects the random variations in the interconnection strengths, but the value of each connection coefficient is restricted to a set of known modes, and cannot portray the stochastic increase or decrease of the connection strength obeying some random distribution. To quantitatively express the random variation in the connection strengths, we must overcome the restrictions of the Bernoulli distribution and Markov chain. To this end, we propose a randomly varying topology model with the following capabilities: (1) The randomness in the interconnection coefficient between any two adjacent sensor nodes is quantifiably described; (2) The interconnection coefficient is decoupled with its statistical information, enabling the smooth computation of the event-triggered distributed filter gain. Unrestricted expression of the random interconnections in

a sensor network is the second main motivator of the present study.

Summarizing the above considerations, we attempt to newly design an event-based distributed H_∞ filter for one-sided Lipshitz type nonlinear systems with a random sensor network topology under fading measurements. The primary contributions of the present research are threefold. (1) The system plant model is perturbed by a one-sided Lipschitz nonlinearity, which generalizes the normal Lipschitz nonlinear constraint. (2) The topology is randomly varying and the interconnection coefficients between adjacent nodes are described by multiplicative stochastic processes. The resulting filtering error dynamics contain randomly varying parameters. (3) The statistical information of the interconnection strengths is decoupled from the filter gain parameter by matrix factorization. The event-triggered distributed H_∞ filter gain is effectively calculated by a convex optimization method. Moreover, the bandwidth occupancy rates of the communication network are alleviated by an event-triggered scheduling strategy.

Notations. The notations adopted in this paper are generally standard. The set of $n \times m$ matrices is denoted as $\mathbb{R}^{n\times m}$. $A \otimes B$ is the Kronecker product of matrices A and B. For matrix P, its inverse and transpose are indicated by the notations P^{-1} and P^{T}, respectively. $\mathrm{diag}\{N_1, N_2, \ldots, N_n\}$ refers to a block-diagonal matrix. For stochastic variable x, $\mathrm{E}\{x\}$ represents its mathematical expectation. $\|\cdot\|$ is the Euclidean norm. The notation $\langle\cdot\rangle$ designates the inner product. In a symmetric matrix, the asterisk $*$ stands for a symmetric term.

2 Problem formulation and preliminaries

2.1 Plant model and random topology structure

Consider the nonlinear system shown as

$$\begin{cases} x(k+1) = Ax(k) + f(k, x(k)) + B\nu(k), \\ z(k) = Hx(k), \end{cases} \tag{1}$$

where $x(k) \in \mathbb{R}^{n_x}$ is the state vector of the target plant, $z(k) \in \mathbb{R}^{n_z}$ is the output signal to be estimated, and $\nu(k) \in \mathbb{R}^{n_v}$ is the external disturbance input belonging to $l_2[0, +\infty)$. A, B, and H are real constant matrices of appropriate dimensions. $f(k, x(k))$ is the nonlinear perturbation satisfying the following one-sided Lipschitz constraint.

Assumption 1. For any $u, v \in \mathbb{R}^{n_x}$, there exists a scalar ρ satisfying

$$\langle f(k, u) - f(k, v), u - v\rangle \leqslant \rho \|u - v\|^2, \tag{2}$$

where the scalar ρ is called as the one-sided Lipschitz constant.

Assumption 2. For any $u, v \in \mathbb{R}^{n_x}$, there exist scalars $\theta,\ \phi$ such that

$$[f(k, u) - f(k, v)]^{\mathrm{T}} [f(k, u) - f(k, v)] \leqslant \phi \|u - v\|^2 + \theta \langle u - v, f(k, u) - f(k, v)\rangle \tag{3}$$

and the nonlinear function $f(k, x(k))$ is correspondingly said to be quadratically inner-bounded.

Remark 1. This paper takes into consideration the nonlinear perturbed function $f(k, x(k))$ satisfying one-sided Lipschitz condition. Obviously, the scalars ρ, θ, ϕ are not restricted to be positive as in conventional Lipschitz condition [33]. That is, they can also be chosen to be zero or even negative. On the other hand, when $\theta > 0$, $\phi = 0$ the one-sided Lipschitz condition will reduce to the standard Lipschitz one, or any normal Lipschitz condition is only a specific case of one-sided one. Furthermore, just as pointed out in [34], different from the one-sided condition in (2), the two-sided inequality $-l\|u-v\|^2 \leqslant \langle f(k, u) - f(k, v), u - v\rangle \leqslant l\|u - v\|^2$ holds for standard Lipschitz nonlinearity with scalar $l > 0$.

This paper is concerned with the distributed filter design for system (1). The measurement signal from the given sensor network is described as

$$y_i(k) = \alpha_i(k)C_i x(k) + D_i\nu(k), \tag{4}$$

where $y_i(k) \in \mathbb{R}^{n_y}$ $(i \in \mathcal{N} = \{1, 2, \ldots, N\})$ is the measurement output vector of the plant from the i-th sensor node, and compatibly dimensional matrices C_i, D_i are real and known. $\alpha_i(k) \in [0, 1]$ is a random sequence, which is used to portray the probabilistic characteristics of fading measurements with the first

and second moments as $\mathrm{E}\{\alpha_i(k)\} = \bar{\alpha}_i$ and $\mathrm{E}\{(\alpha_i(k) - \bar{\alpha}_i)^2\} = \alpha_i^*$, respectively, where $\bar{\alpha}_i$ and α_i^* are known scalars.

For a sensor network consisting of N nodes, its topology is expressed by a directed graph $\mathcal{G} = (\mathcal{N}, \mathcal{E}, \mathbb{C})$, where the set of sensor nodes is denoted by $\mathcal{N}$, the set of edges is represented as $\mathcal{E} \subseteq \mathcal{N} \times \mathcal{N}$, and $\mathbb{C}=[a_{ij}^k]_{N\times N}$ $(i,\ j \in \mathcal{N})$ stands for the weighted adjacency matrix with interconnection element $a_{ij}^k \geqslant 0$ at time instant k. $a_{ij}^k > 0$ indicates that the sensor node i can obtain information transmitted from the node j. It is assumed that a_{ii}^k=1 for all $i \in \mathcal{N}$. The adjacent node set of the sensor node i is indicated by $\mathcal{N}_i = \{j \in \mathcal{N} \mid j \neq i; i, j \in \mathcal{N}\}$.

In this paper, we will be devoted to the randomly varying topology structure caused by the variations of running surroundings and environments. The random change of interconnection coefficient a_{ij}^k $(i \in \mathcal{N}, j \in \mathcal{N}_i)$ is given by

$$a_{ij}^k = \beta_{ij}^k c_{ij}, \tag{5}$$

where $c_{ij} \geqslant 0$ is a scalar, and $\beta_{ij}^k \in [0, 1]$ is a random sequence used to reflect the probabilistic property of interconnection coefficient between the nodes i and j with $\mathrm{E}\{\beta_{ij}^k\} = \bar{\beta}_{ij}$ and $\mathrm{E}\{(\beta_{ij}^k - \bar{\beta}_{ij})^2\} = \beta_{ij}^*$, where $\bar{\beta}_{ij}$ and β_{ij}^* are known scalars.

Remark 2. As stated in [45], the multiplicative perturbation form is frequently used to describe the topology structure variation [45,47,48]. Thus, different from the random topology variation described by Bernoulli distributed variable and Markov chains [39–41,43,46], the multiplicative stochastic description (5) is presented in this paper to reflect the random reality of each interconnection coefficient a_{ij}^k. Compared with the expression by simply assuming the connection coefficient a_{ij}^k in (5) as a random variable with known probabilistic properties, a_{ij}^k in (5) is decomposed as the product of the deterministic constant c_{ij} (representing the modulus of connection strength) and its random factor β_{ij}^k, where β_{ij}^k obeys any random distribution within the interval $[0, 1]$.

2.2 Distributed filtering based on event-triggered scheme

The following distributed filter is constructed in this paper:

$$\begin{cases} \hat{x}_i(k+1) = A\hat{x}_i(k) + f(k, \hat{x}_i(k)) + L_{ii}[y_i(k) - \bar{\alpha}_i C_i \hat{x}_i(k)] + \displaystyle\sum_{j\in\mathcal{N}_i} a_{ij}^k L_{ij}[y_j(k) - \bar{\alpha}_j C_j \hat{x}_j(k)], \\ \hat{z}_i(k) = H\hat{x}_i(k), \end{cases} \tag{6}$$

where $\hat{x}_i(k) \in \mathbb{R}^{n_x}$ is the estimate of vector $x(k)$ from the sensor node i, $\hat{z}_i(k) \in \mathbb{R}^{n_z}$ represents the estimate of vector $z_i(k)$ from the filter node i, and L_{ii} and L_{ij} $(i \in \mathcal{N}, j \in \mathcal{N}_i)$ are the filter gain matrices to be designed later.

Meanwhile, to alleviate the communication resource burdens and save the sensor nodes' energy costs used to send measurement signals, the event-triggered transmission mechanism is adopted.

The last event triggering time instant of node i is denoted by t_s^i $(i \in \mathcal{N}, s = 0, 1, 2, \ldots)$, and then $y_i(t_s^i)$ is the measurement signal transmitted at time instant t_s^i. The next triggering instant t_{s+1}^i can be recursively obtained by

$$t_{s+1}^i = \min_{k>t_s^i} \left\{k | g_i^{\mathrm{T}}(k) g_i(k) \geqslant \sigma_i y_i^{\mathrm{T}}(k) y_i(k)\right\}, \tag{7}$$

where $g_i(k) = y_i(k) - y_i(t_s^i)$ and $\sigma_i > 0$ is the triggering threshold.

Based on the above event-triggered transmission protocol, for any $k \in [t_s^i, t_{s+1}^i)$, the first equation of (6) reads as

$$\begin{aligned} \hat{x}_i(k+1) = {} & A\hat{x}_i(k) + f(k, \hat{x}_i(k)) + L_{ii}[\alpha_i(k) C_i x(k) + D_i \nu(k) - g_i(k) - \bar{\alpha}_i C_i \hat{x}_i(k)] \\ & + \sum_{j\in\mathcal{N}_i} \beta_{ij}^k c_{ij} L_{ij}[\alpha_j(k) C_j x(k) + D_j \nu(k) - g_j(k) - \bar{\alpha}_j C_j \hat{x}_j(k)]. \end{aligned} \tag{8}$$

In what follows, the following simplified notations are utilized:

$$\begin{aligned}
&\tilde{x}(k)=[\tilde{x}_1^{\mathrm{T}}(k)\ \tilde{x}_2^{\mathrm{T}}(k)\ \cdots\ \tilde{x}_N^{\mathrm{T}}(k)]^{\mathrm{T}},\ \tilde{z}(k)=[\tilde{z}_1^{\mathrm{T}}(k)\ \tilde{z}_2^{\mathrm{T}}(k)\ \cdots\ \tilde{z}_N^{\mathrm{T}}(k)]^{\mathrm{T}},\ \bar{L}=[c_{ij}L_{ij}]_{N\times N},\\
&\hat{L}=\mathrm{diag}\{L_{11},L_{22},\ldots,L_{NN}\},\ \Delta_L(k)=[\beta_{ij}^k c_{ij}L_{ij}]_{N\times N},\ \Delta_L=[\bar{\beta}_{ij}c_{ij}L_{ij}]_{N\times N},\\
&\Gamma=\mathrm{diag}\{\bar{\alpha}_1 I_{n_y},\bar{\alpha}_2 I_{n_y},\ldots,\bar{\alpha}_N I_{n_y}\},\ \Gamma(k)=\mathrm{diag}\{\alpha_1(k)I_{n_y},\alpha_2(k)I_{n_y},\ldots,\alpha_N(k)I_{n_y}\},\\
&\tilde{F}=[\tilde{f}_1^{\mathrm{T}}\ \tilde{f}_2^{\mathrm{T}}\ \cdots\ \tilde{f}_N^{\mathrm{T}}]^{\mathrm{T}},\ g(k)=[g_1^{\mathrm{T}}(k)\ g_2^{\mathrm{T}}(k)\ \cdots\ g_N^{\mathrm{T}}(k)]^{\mathrm{T}},\ \bar{C}=[C_1^{\mathrm{T}}\ C_2^{\mathrm{T}}\ \cdots\ C_N^{\mathrm{T}}]^{\mathrm{T}},\\
&\tilde{C}=\mathrm{diag}\{C_1,C_2,\ldots,C_N\},\ \bar{D}=[D_1^{\mathrm{T}}\ D_2^{\mathrm{T}}\ \cdots\ D_N^{\mathrm{T}}]^{\mathrm{T}},\\
&\bar{B}=[\underbrace{B^{\mathrm{T}}\ B^{\mathrm{T}}\ \cdots\ B^{\mathrm{T}}}_{N}]^{\mathrm{T}},\ \bar{H}=\mathrm{diag}\{\underbrace{H,H,\ldots,H}_{N}\}.
\end{aligned}\tag{9}$$

Subsequently, by letting $\tilde{x}_i(k)=x(k)-\hat{x}_i(k)$ and $\tilde{f}_i=f(k,x(k))-f(k,\hat{x}_i(k))$, the compact form of filtering error dynamics represents as follows:

$$\begin{cases}
\tilde{x}(k+1)=[I_N\otimes A-\hat{L}\Gamma\tilde{C}-\Delta_L\Gamma\tilde{C}-(\Delta_L(k)-\Delta_L)\Gamma\tilde{C}]\tilde{x}(k)\\
\qquad\qquad -[\hat{L}(\Gamma(k)-\Gamma)\bar{C}+(\Delta_L(k)-\Delta_L)(\Gamma(k)-\Gamma)\bar{C}+\Delta_L(\Gamma(k)-\Gamma)\bar{C}]x(k)\\
\qquad\qquad +[\bar{B}-\hat{L}\bar{D}-(\Delta_L(k)-\Delta_L)\bar{D}-\Delta_L\bar{D}]\nu(k)+[\hat{L}+(\Delta_L(k)-\Delta_L)+\Delta_L]g(k)+\tilde{F},\\
\tilde{z}(k)=\bar{H}\tilde{x}(k).
\end{cases}\tag{10}$$

By letting $\eta(k)=[x^{\mathrm{T}}(k)\ \tilde{x}^{\mathrm{T}}(k)]^{\mathrm{T}}$ and $\bar{z}(k)=[z^{\mathrm{T}}(k)\ \tilde{z}^{\mathrm{T}}(k)]^{\mathrm{T}}$, the filtering error system can be written as follows:

$$\begin{cases}
\eta(k+1)=(\mathcal{A}-\mathcal{C})\eta(k)+\mathcal{F}+(\mathcal{B}-\mathcal{D})\nu(k)+(\mathcal{J}-\mathcal{G})g(k),\\
\bar{z}(k)=\mathcal{H}\eta(k),
\end{cases}\tag{11}$$

where

$$\mathcal{A}=\begin{bmatrix}A & 0\\ 0 & \Theta_1\end{bmatrix},\ \mathcal{C}=\begin{bmatrix}0 & 0\\ \Theta_2 & \Theta_3\end{bmatrix},\ \mathcal{F}=\begin{bmatrix}f(k,x(k))\\ \tilde{F}\end{bmatrix},\ \mathcal{B}=\begin{bmatrix}B\\ \Theta_4\end{bmatrix},$$
$$\mathcal{D}=\begin{bmatrix}0\\ \Theta_5\end{bmatrix},\ \mathcal{J}=\begin{bmatrix}0\\ \Theta_6\end{bmatrix},\ \mathcal{G}=\begin{bmatrix}0\\ \Theta_7\end{bmatrix},\ \mathcal{H}=\begin{bmatrix}H & 0\\ 0 & \bar{H}\end{bmatrix}$$

with

$$\begin{aligned}
&\Theta_1=I_N\otimes A-\hat{L}\Gamma\tilde{C}-\Delta_L\Gamma\tilde{C},\ \Theta_2=\hat{L}(\Gamma(k)-\Gamma)\bar{C}+(\Delta_L(k)-\Delta_L)(\Gamma(k)-\Gamma)\bar{C}+\Delta_L(\Gamma(k)-\Gamma)\bar{C},\\
&\Theta_3=(\Delta_L(k)-\Delta_L)\Gamma\tilde{C},\ \Theta_4=\bar{B}-\hat{L}\bar{D}-\Delta_L\bar{D},\ \Theta_5=(\Delta_L(k)-\Delta_L)\bar{D},\\
&\Theta_6=\hat{L}+\Delta_L,\ \Theta_7=-(\Delta_L(k)-\Delta_L).
\end{aligned}$$

Remark 3. Due to the existence of the stochastic terms $\mathcal{C}$, $\mathcal{D}$, and $\mathcal{G}$, Eq. (11) is actually a dynamical system with randomly varying parameters. It can be seen that the stochastic parameters result from two random variables, i.e., β_{ij}^k reflecting the random topology variation and $\alpha_i(k)$ describing the fading measurements phenomenon, respectively.

2.3 Definitions and the main objective

Some basic definitions and the main goal of this paper are presented in the following.

Definition 1. The augmented system (11) is exponentially stable in mean square sense if, under $\nu(k)\equiv 0$ and initial condition $\eta(0)$, we have $\mathrm{E}\{\|\eta(k)\|^2\}\leqslant\varsigma\delta^k\|\eta(0)\|^2$, where $\varsigma>0$ and $0<\delta<1$ are scalars.

Definition 2. Eq. (8) is called a distributed H_∞ filter of the nonlinear system (1) with Assumptions 1 and 2 under the event-triggered communication protocol (7), if the augmented system (11) with $\nu(k)=0$ is exponentially stable in mean square sense, and under the zero-initial condition, the H_∞ performance constraint in the following is satisfied for any nonzero disturbance $\nu(k)$:

$$\sum_{k=0}^{\infty}\mathrm{E}\{\|\bar{z}(k)\|^2\}\leqslant\gamma^2\sum_{k=0}^{\infty}\|\nu(k)\|^2,$$

where the specified scalar $\gamma>0$ indicates the disturbance attenuation degree.

Now, the main purpose of this paper can be stated as follows. For system (1) with the one-sided Lipschitz nonlinearity satisfying (2) and (3), the randomly varying topology characterized by (5), and the imperfect measurement portrayed by (4), we aim to construct an event-triggered distributed H_∞ filter with the form of (8) such that (i) the augmented system (11) with $\nu(k)=0$ is exponentially stable in mean square sense; and (ii) the H_∞ performance constraint in Definition 2 is satisfied for any nonzero disturbance $\nu(k)$.

3 Main results

This section will present the stochastic bounded real lemma (BRL) of the filtering error dynamics (11). Then the design method will be provided for the event-triggered distributed filter (8).

3.1 Bounded real lemma

The following abbreviations are adopted in the sequel, for the sake of notational simplification:

$$\bar{\mathcal{C}}_1=\mathrm{diag}\{(\bar{\Gamma}\bar{C})^{\mathrm{T}}\Upsilon(\bar{\Gamma}\bar{C}),0\},\ \bar{\mathcal{C}}_2=\mathrm{diag}\{(\Gamma\bar{C})^{\mathrm{T}}\Upsilon(\Gamma\bar{C}),0\},$$
$$\bar{\Gamma}=\mathrm{diag}\{\sqrt{\alpha_1^*}I_{n_y},\sqrt{\alpha_2^*}I_{n_y},\ldots,\sqrt{\alpha_N^*}I_{n_y}\},\ \Upsilon=\mathrm{diag}\{\sigma_1I_{n_y},\sigma_2I_{n_y},\ldots,\sigma_NI_{n_y}\},$$
$$\tilde{\mathcal{D}}=\begin{bmatrix}0\\ \bar{L}_1\bar{D}\end{bmatrix},\ \tilde{\mathcal{G}}=\begin{bmatrix}0\\ \bar{L}_1\end{bmatrix},\ \tilde{\mathcal{C}}=\begin{bmatrix}0 & 0\\ 0 & \bar{L}_1\Gamma\tilde{C}\end{bmatrix},\ \hat{\mathcal{C}}_i=\begin{bmatrix}0 & 0\\ \sqrt{\alpha_i^*}\hat{L}e_iC_i & 0\end{bmatrix},$$
$$\mathcal{C}_{i1}=\begin{bmatrix}0 & 0\\ \sqrt{\alpha_i^*}\bar{L}_1e_iC_i & 0\end{bmatrix},\ \mathcal{C}_{i2}=\begin{bmatrix}0 & 0\\ \sqrt{\alpha_i^*}\bar{L}_2e_iC_i & 0\end{bmatrix},\ e_i=[\underbrace{0_{n_y},\ldots,}_{i-1}I_{n_y},\underbrace{\ldots,0_{n_y}}_{N-i}]^{\mathrm{T}},$$
$$\bar{L}_1=\left[\sqrt{\beta_{ij}^*}c_{ij}L_{ij}\right]_{N\times N},\ \bar{L}_2=\Delta_L=[\bar{\beta}_{ij}c_{ij}L_{ij}]_{N\times N}.$$

We now can present the following stochastic BRL for system (11).

Theorem 1. Given a scalar $\gamma>0$, system (11) is exponentially stable in the mean square sense and achieves the H_∞ performance constraint in Definition 2, if there exist diagonal matrices $P_j>0$ ($j=1,2,\ldots,N+1$) and scalars $\varepsilon_1>0,\ \varepsilon_2>0$ satisfying $\mathcal{P}\triangleq\mathrm{diag}\{P_1,\mathcal{P}_2\}=\mathrm{diag}\{P_1,P_2,P_3,\ldots,P_{N+1}\}>0$ and

$$\hat{\Lambda}=\begin{bmatrix}\hat{\chi}_{11} & \hat{\chi}_{12} & \hat{\chi}_{13} & \hat{\chi}_{14}\\ * & \hat{\chi}_{22} & \hat{\chi}_{23} & \hat{\chi}_{24}\\ * & * & \hat{\chi}_{33} & \hat{\chi}_{34}\\ * & * & * & \hat{\chi}_{44}\end{bmatrix}<0, \tag{12}$$

where

$$\hat{\chi}_{11}=\mathcal{A}^{\mathrm{T}}\mathcal{P}\mathcal{A}-\mathcal{P}+\sum_{i=1}^{N}(\hat{\mathcal{C}}_i^{\mathrm{T}}\mathcal{P}\hat{\mathcal{C}}_i+\mathcal{C}_{i1}^{\mathrm{T}}\mathcal{P}\mathcal{C}_{i1}+\mathcal{C}_{i2}^{\mathrm{T}}\mathcal{P}\mathcal{C}_{i2})+\tilde{\mathcal{C}}^{\mathrm{T}}\mathcal{P}\tilde{\mathcal{C}}+\varepsilon_1\rho I+\varepsilon_2\phi I+\bar{\mathcal{C}}_1+\bar{\mathcal{C}}_2+\mathcal{H}^{\mathrm{T}}\mathcal{H},$$
$$\hat{\chi}_{12}=\mathcal{A}^{\mathrm{T}}\mathcal{P}-\frac{\varepsilon_1 I}{2}+\frac{\varepsilon_2\theta I}{2},\ \hat{\chi}_{13}=\mathcal{A}^{\mathrm{T}}\mathcal{P}\mathcal{J}-\tilde{\mathcal{C}}^{\mathrm{T}}\mathcal{P}\tilde{\mathcal{G}},\ \hat{\chi}_{14}=\mathcal{A}^{\mathrm{T}}\mathcal{P}\mathcal{B}+\tilde{\mathcal{C}}^{\mathrm{T}}\mathcal{P}\tilde{\mathcal{D}},\ \hat{\chi}_{22}=\mathcal{P}-\varepsilon_2 I,\ \hat{\chi}_{23}=\mathcal{P}\mathcal{J},$$
$$\hat{\chi}_{24}=\mathcal{P}\mathcal{B},\ \hat{\chi}_{33}=\mathcal{J}^{\mathrm{T}}\mathcal{P}\mathcal{J}+\tilde{\mathcal{G}}^{\mathrm{T}}\mathcal{P}\tilde{\mathcal{G}}-I,\ \hat{\chi}_{34}=\mathcal{J}^{\mathrm{T}}\mathcal{P}\mathcal{B}-\tilde{\mathcal{G}}^{\mathrm{T}}\mathcal{P}\tilde{\mathcal{D}},\ \hat{\chi}_{44}=\mathcal{B}^{\mathrm{T}}\mathcal{P}\mathcal{B}+\tilde{\mathcal{D}}^{\mathrm{T}}\mathcal{P}\tilde{\mathcal{D}}-\gamma^2I.$$

Proof. This proof procedure includes two steps. In step 1, the exponential stability in mean square sense of system (11) ($\nu(k)=0$) is shown, and then the stochastic BRL of system (11) with any nonzero $\nu(k)$ is obtained.

Step 1. Select the Lyapunov function as $V(k)=\eta^{\mathrm{T}}(k)\mathcal{P}\eta(k)$ with $\mathcal{P}=\mathrm{diag}\{P_1,P_2,\ldots,P_{N+1}\}>0$.

For system (11) ($\nu(k)=0$), calculate the expectation of forward difference of $V(k)$, defined as $\Delta V(k)\triangleq V(k+1)-V(k)$, that is

$$\begin{aligned}&\mathrm{E}\{\Delta V(k)\}\\ &=\mathrm{E}\big\{\big[(\mathcal{A}-\mathcal{C})\eta(k)+\mathcal{F}+(\mathcal{J}-\mathcal{G})g(k)\big]^{\mathrm{T}}\mathcal{P}\big[(\mathcal{A}-\mathcal{C})\eta(k)+\mathcal{F}+(\mathcal{J}-\mathcal{G})g(k)\big]-\eta^{\mathrm{T}}(k)\mathcal{P}\eta(k)\big\}\end{aligned}$$

$$= \mathrm{E}\{\eta^{\mathrm{T}}(k)(\mathcal{A}^{\mathrm{T}}\mathcal{P}\mathcal{A}+\mathcal{C}^{\mathrm{T}}\mathcal{P}\mathcal{C}-\mathcal{P})\eta(k)+2\eta^{\mathrm{T}}(k)\mathcal{A}^{\mathrm{T}}\mathcal{P}\mathcal{F}+2\eta^{\mathrm{T}}(k)(\mathcal{A}^{\mathrm{T}}\mathcal{P}\mathcal{J}+\mathcal{C}^{\mathrm{T}}\mathcal{P}\mathcal{G})g(k) + \mathcal{F}^{\mathrm{T}}\mathcal{P}\mathcal{F}+2\mathcal{F}^{\mathrm{T}}\mathcal{P}\mathcal{J}g(k)+g^{\mathrm{T}}(k)(\mathcal{J}^{\mathrm{T}}\mathcal{P}\mathcal{J}+\mathcal{G}^{\mathrm{T}}\mathcal{P}\mathcal{G})g(k)\}. \tag{13}$$

In the meanwhile, we can obtain

$$\mathrm{E}\{\eta^{\mathrm{T}}(k)\mathcal{C}^{\mathrm{T}}\mathcal{P}\mathcal{C}\eta(k)\} = \mathrm{E}\{x^{\mathrm{T}}(k)\Theta_2^{\mathrm{T}}\mathcal{P}_2\Theta_2x(k)+\tilde{x}^{\mathrm{T}}(k)\Theta_3^{\mathrm{T}}\mathcal{P}_2\Theta_3\tilde{x}(k)\}, \tag{14}$$

and its first term $\mathrm{E}\{x^{\mathrm{T}}(k)\Theta_2^{\mathrm{T}}\mathcal{P}_2\Theta_2x(k)\}$ is computed as

$$\begin{aligned}&\mathrm{E}\{x^{\mathrm{T}}(k)\Theta_2^{\mathrm{T}}\mathcal{P}_2\Theta_2x(k)\}\\ &= \mathrm{E}\{x^{\mathrm{T}}(k)[((\Delta_L(k)-\Delta_L)(\Gamma(k)-\Gamma)\bar{C})^{\mathrm{T}}\mathcal{P}_2((\Delta_L(k)-\Delta_L)(\Gamma(k)-\Gamma)\bar{C})\\ &\quad+(\Delta_L(\Gamma(k)-\Gamma)\bar{C})^{\mathrm{T}}\mathcal{P}_2(\Delta_L(\Gamma(k)-\Gamma)\bar{C})+(\hat{L}(\Gamma(k)-\Gamma)\bar{C})^{\mathrm{T}}\mathcal{P}_2(\hat{L}(\Gamma(k)-\Gamma)\bar{C})]x(k)\}.\end{aligned} \tag{15}$$

Moreover, we can also deduce that

$$\begin{aligned}&\mathrm{E}\{x^{\mathrm{T}}(k)((\Delta_L(k)-\Delta_L)(\Gamma(k)-\Gamma)\bar{C})^{\mathrm{T}}\mathcal{P}_2((\Delta_L(k)-\Delta_L)(\Gamma(k)-\Gamma)\bar{C})x(k)\}\\ &= \mathrm{E}\left\{x^{\mathrm{T}}(k)\sum_{i=1}^{N}\sum_{j\in\mathcal{N}_i}(\beta_{ij}(k)-\bar{\beta}_{ij})^2(\alpha_j(k)-\bar{\alpha}_j)^2c_{ij}^2(L_{ij}C_j)^{\mathrm{T}}P_{i+1}(L_{ij}C_j)x(k)\right\}\\ &= \mathrm{E}\left\{\eta^{\mathrm{T}}(k)\sum_{i=1}^{N}\mathcal{C}_{i1}^{\mathrm{T}}\mathcal{P}\mathcal{C}_{i1}\eta(k)\right\}.\end{aligned} \tag{16}$$

At the same time, it is not difficult to verify that

$$\begin{aligned}&\mathrm{E}\{x^{\mathrm{T}}(k)(\Delta_L(\Gamma(k)-\Gamma)\bar{C})^{\mathrm{T}}\mathcal{P}_2(\Delta_L(\Gamma(k)-\Gamma)\bar{C})x(k)\} = \mathrm{E}\left\{\eta^{\mathrm{T}}(k)\sum_{i=1}^{N}\mathcal{C}_{i2}^{\mathrm{T}}\mathcal{P}\mathcal{C}_{i2}\eta(k)\right\},\\ &\mathrm{E}\{x^{\mathrm{T}}(k)(\hat{L}(\Gamma(k)-\Gamma)\bar{C})^{\mathrm{T}}\mathcal{P}_2(\hat{L}(\Gamma(k)-\Gamma)\bar{C})x(k)\} = \mathrm{E}\left\{\eta^{\mathrm{T}}(k)\sum_{i=1}^{N}\hat{\mathcal{C}}_i^{\mathrm{T}}\mathcal{P}\hat{\mathcal{C}}_i\eta(k)\right\}.\end{aligned} \tag{17}$$

We can also derive that

$$\mathrm{E}\{\tilde{x}^{\mathrm{T}}(k)\Theta_3^{\mathrm{T}}\mathcal{P}_2\Theta_3\tilde{x}(k)\} = \mathrm{E}\{\tilde{x}^{\mathrm{T}}(k)(\bar{L}_1\Gamma\bar{C})^{\mathrm{T}}\mathcal{P}_2(\bar{L}_1\Gamma\bar{C})\tilde{x}(k)\} = \mathrm{E}\{\eta^{\mathrm{T}}(k)\tilde{\mathcal{C}}^{\mathrm{T}}\mathcal{P}\tilde{\mathcal{C}}\eta(k)\}. \tag{18}$$

In terms of (14)–(18), it is easy to see

$$\begin{aligned}\mathrm{E}\{\eta^{\mathrm{T}}(k)\mathcal{C}^{\mathrm{T}}\mathcal{P}\mathcal{C}\eta(k)\} &= \mathrm{E}\{x^{\mathrm{T}}(k)\Theta_2^{\mathrm{T}}\mathcal{P}_2\Theta_2x(k)+\tilde{x}^{\mathrm{T}}(k)\Theta_3^{\mathrm{T}}\mathcal{P}_2\Theta_3\tilde{x}(k)\}\\ &= \mathrm{E}\left\{\eta^{\mathrm{T}}(k)\left[\sum_{i=1}^{N}(\hat{\mathcal{C}}_i^{\mathrm{T}}\mathcal{P}\hat{\mathcal{C}}_i+\mathcal{C}_{i1}^{\mathrm{T}}\mathcal{P}\mathcal{C}_{i1}+\mathcal{C}_{i2}^{\mathrm{T}}\mathcal{P}\mathcal{C}_{i2})+\tilde{\mathcal{C}}^{\mathrm{T}}\mathcal{P}\tilde{\mathcal{C}}\right]\eta(k)\right\}.\end{aligned} \tag{19}$$

Similarly, we straightly find that

$$\mathrm{E}\{g^{\mathrm{T}}(k)\mathcal{G}^{\mathrm{T}}\mathcal{P}\mathcal{G}g(k)\} = \mathrm{E}\{g^{\mathrm{T}}(k)\tilde{\mathcal{G}}^{\mathrm{T}}\mathcal{P}\tilde{\mathcal{G}}g(k)\},\ \mathrm{E}\{\eta^{\mathrm{T}}(k)\mathcal{C}^{\mathrm{T}}\mathcal{P}\mathcal{G}g(k)\} = \mathrm{E}\{-\eta^{\mathrm{T}}(k)\tilde{\mathcal{C}}^{\mathrm{T}}\mathcal{P}\tilde{\mathcal{G}}g(k)\}. \tag{20}$$

In view of the above derivations, we then get

$$\begin{aligned}\mathrm{E}\{\Delta V(k)\} \leqslant \mathrm{E}\Bigg\{&\eta^{\mathrm{T}}(k)\left[\mathcal{A}^{\mathrm{T}}\mathcal{P}\mathcal{A}-\mathcal{P}+\tilde{\mathcal{C}}^{\mathrm{T}}\mathcal{P}\tilde{\mathcal{C}}+\sum_{i=1}^{N}(\hat{\mathcal{C}}_i^{\mathrm{T}}\mathcal{P}\hat{\mathcal{C}}_i+\mathcal{C}_{i1}^{\mathrm{T}}\mathcal{P}\mathcal{C}_{i1}+\mathcal{C}_{i2}^{\mathrm{T}}\mathcal{P}\mathcal{C}_{i2})\right]\eta(k)\\ &+2\eta^{\mathrm{T}}(k)\mathcal{A}^{\mathrm{T}}\mathcal{P}\mathcal{F}+\mathcal{F}^{\mathrm{T}}\mathcal{P}\mathcal{F}+2\mathcal{F}^{\mathrm{T}}\mathcal{P}\mathcal{J}g(k)+2\eta^{\mathrm{T}}(k)(\mathcal{A}^{\mathrm{T}}\mathcal{P}\mathcal{J}-\tilde{\mathcal{C}}^{\mathrm{T}}\mathcal{P}\tilde{\mathcal{G}})g(k)\\ &+g^{\mathrm{T}}(k)(\tilde{\mathcal{G}}^{\mathrm{T}}\mathcal{P}\tilde{\mathcal{G}}+\mathcal{J}^{\mathrm{T}}\mathcal{P}\mathcal{J})g(k)\Bigg\}.\end{aligned} \tag{21}$$

From (7), it follows that

$$-g^{\mathrm{T}}(k)g(k)+(\Gamma(k)\bar{C}x(k))^{\mathrm{T}}\Upsilon(\Gamma(k)\bar{C}x(k))\geqslant 0. \tag{22}$$

As a consequence, we then arrive at

$$\begin{aligned}&\mathrm{E}\{-g^{\mathrm{T}}(k)g(k)+(\Gamma(k)\bar{C}x(k))^{\mathrm{T}}\Upsilon(\Gamma(k)\bar{C}x(k))\}\\&=\mathrm{E}\{-g^{\mathrm{T}}(k)g(k)+x^{\mathrm{T}}(k)(\bar{\Gamma}\bar{C})^{\mathrm{T}}\Upsilon(\bar{\Gamma}\bar{C})x(k)+x^{\mathrm{T}}(k)(\Gamma\bar{C})^{\mathrm{T}}\Upsilon(\Gamma\bar{C})x(k)\}\\&=\mathrm{E}\{-g^{\mathrm{T}}(k)g(k)+\eta^{\mathrm{T}}(k)\bar{\mathcal{C}}_1\eta(k)+\eta^{\mathrm{T}}(k)\bar{\mathcal{C}}_2\eta(k)\}.\end{aligned}\tag{23}$$

The following can be yielded by taking (23) into consideration:

$$\begin{aligned}\mathrm{E}\{\Delta V(k)\}\leqslant\mathrm{E}\Bigg\{&\eta^{\mathrm{T}}(k)\left[\mathcal{A}^{\mathrm{T}}\mathcal{P}\mathcal{A}-\mathcal{P}+\tilde{\mathcal{C}}^{\mathrm{T}}\mathcal{P}\tilde{\mathcal{C}}+\bar{\mathcal{C}}_1+\bar{\mathcal{C}}_2)+\sum_{i=1}^{N}(\hat{\mathcal{C}}_i^{\mathrm{T}}\mathcal{P}\hat{\mathcal{C}}_i+\mathcal{C}_{i1}^{\mathrm{T}}\mathcal{P}\mathcal{C}_{i1}+\mathcal{C}_{i2}^{\mathrm{T}}\mathcal{P}\mathcal{C}_{i2})\right]\eta(k)\\&+2\eta^{\mathrm{T}}(k)\mathcal{A}^{\mathrm{T}}\mathcal{P}\mathcal{F}+\mathcal{F}^{\mathrm{T}}\mathcal{P}\mathcal{F}+2\mathcal{F}^{\mathrm{T}}\mathcal{P}\mathcal{J}g(k)+2\eta^{\mathrm{T}}(k)(\mathcal{A}^{\mathrm{T}}\mathcal{P}\mathcal{J}-\tilde{\mathcal{C}}^{\mathrm{T}}\mathcal{P}\tilde{\mathcal{G}})g(k)\\&+g^{\mathrm{T}}(k)(\tilde{\mathcal{G}}^{\mathrm{T}}\mathcal{P}\tilde{\mathcal{G}}+\mathcal{J}^{\mathrm{T}}\mathcal{P}\mathcal{J}-I)g(k)\Bigg\}.\end{aligned}\tag{24}$$

Select an augmented vector as $\xi(k)=[\eta^{\mathrm{T}}(k)\ \mathcal{F}^{\mathrm{T}}\ g^{\mathrm{T}}(k)]^{\mathrm{T}}$. Recalling Assumption 1 results in $\rho\eta^{\mathrm{T}}(k)\eta(k)-\eta^{\mathrm{T}}(k)\mathcal{F}\geqslant 0$. Hence, for any $\varepsilon_1>0$, it is true that

$$\varepsilon_1\xi^{\mathrm{T}}(k)\begin{bmatrix}\rho I & -\dfrac{I}{2} & 0\\ * & 0 & 0\\ * & * & 0\end{bmatrix}\xi(k)\geqslant 0.\tag{25}$$

In addition, Assumption 2 implies that for any $\varepsilon_2>0$ there is

$$\varepsilon_2\xi^{\mathrm{T}}(k)\begin{bmatrix}\phi I & \dfrac{\theta I}{2} & 0\\ * & -I & 0\\ * & * & 0\end{bmatrix}\xi(k)\geqslant 0.\tag{26}$$

Then, it can be observed from (24)–(26) that

$$\mathrm{E}\{\Delta V(k)\}\leqslant\mathrm{E}\{\xi^{\mathrm{T}}(k)\bar{\Lambda}\xi(k)\},\tag{27}$$

where

$$\bar{\Lambda}=\begin{bmatrix}\hat{\chi}_{11}-\mathcal{H}^{\mathrm{T}}\mathcal{H} & \hat{\chi}_{12} & \hat{\chi}_{13}\\ * & \hat{\chi}_{22} & \hat{\chi}_{23}\\ * & * & \hat{\chi}_{33}\end{bmatrix}.$$

As we can see, Eq. (12) guarantees $\bar{\Lambda}<0$ according to Schur complements lemma.

Consequently, there is $\mathrm{E}\{\Delta V(k)\}<0$, which implies that there surely is a scalar $\delta\in(0,1)$ satisfying $\mathrm{E}\{V(k+1)\}\leqslant\delta\mathrm{E}\{V(k)\}$. Applying the above inequality directly gives $\mathrm{E}\{V(k)\}\leqslant\delta^k V(0)$. Noticing the Lyapunov function, we further arrive at $\lambda_{\min}(\mathcal{P})\mathrm{E}\{\|\eta(k)\|^2\}\leqslant\lambda_{\max}(\mathcal{P})\delta^k\|\eta(0)\|^2$.

So, for any initial condition $\eta(0)$, we eventually obtain $\mathrm{E}\{\|\eta(k)\|^2\}\leqslant\varsigma\delta^k\|\eta(0)\|^2$ where $\varsigma=\frac{\lambda_{\max}(\mathcal{P})}{\lambda_{\min}(\mathcal{P})}$.

From Definition 1, the error system (11) with $\nu(k)=0$ is exponentially stable in the mean square sense.

Step 2. We now proceed to obtain the stochastic BRL criterion for system (11).

Along system (11) for any nonzero $\nu(k)$, we can compute

$$\begin{aligned}\mathrm{E}\{\Delta V(k)\}=&\mathrm{E}\{[(\mathcal{A}-\mathcal{C})\eta(k)+\mathcal{F}+(\mathcal{J}-\mathcal{G})g(k)+(\mathcal{B}-\mathcal{D})\nu(k)]^{\mathrm{T}}\mathcal{P}[(\mathcal{A}-\mathcal{C})\eta(k)+\mathcal{F}\\&+(\mathcal{J}-\mathcal{G})g(k)+(\mathcal{B}-\mathcal{D})\nu(k)]-\eta^{\mathrm{T}}(k)\mathcal{P}\eta(k)\}\\=&\mathrm{E}\{\eta^{\mathrm{T}}(k)(\mathcal{A}^{\mathrm{T}}\mathcal{P}\mathcal{A}-\mathcal{P}+\mathcal{C}^{\mathrm{T}}\mathcal{P}\mathcal{C})\eta(k)+2\eta^{\mathrm{T}}(k)\mathcal{A}^{\mathrm{T}}\mathcal{P}\mathcal{F}+2\eta^{\mathrm{T}}(k)(\mathcal{A}^{\mathrm{T}}\mathcal{P}\mathcal{J}+\mathcal{C}^{\mathrm{T}}\mathcal{P}\mathcal{G})g(k)\\&+\mathcal{F}^{\mathrm{T}}\mathcal{P}\mathcal{F}+2\mathcal{F}^{\mathrm{T}}\mathcal{P}\mathcal{J}g(k)+g^{\mathrm{T}}(k)(\mathcal{J}^{\mathrm{T}}\mathcal{P}\mathcal{J}+\mathcal{G}^{\mathrm{T}}\mathcal{P}\mathcal{G})g(k)+2\eta^{\mathrm{T}}(k)(\mathcal{A}^{\mathrm{T}}\mathcal{P}\mathcal{B}+\mathcal{C}^{\mathrm{T}}\mathcal{P}\mathcal{D})\nu(k)\\&+2\mathcal{F}^{\mathrm{T}}\mathcal{P}\mathcal{B}\nu(k)+2g^{\mathrm{T}}(k)(\mathcal{J}^{\mathrm{T}}\mathcal{P}\mathcal{B}+\mathcal{G}^{\mathrm{T}}\mathcal{P}\mathcal{D})\nu(k)+\nu^{\mathrm{T}}(k)(\mathcal{D}^{\mathrm{T}}\mathcal{P}\mathcal{D}+\mathcal{B}^{\mathrm{T}}\mathcal{P}\mathcal{B})\nu(k)\}.\end{aligned}\tag{28}$$

On the other hand, it can be observed that

$$\begin{aligned}&\mathrm{E}\{\nu^{\mathrm{T}}(k)\mathcal{D}^{\mathrm{T}}\mathcal{P}\mathcal{D}\nu(k)\}=\mathrm{E}\{\nu^{\mathrm{T}}(k)\tilde{\mathcal{D}}^{\mathrm{T}}\mathcal{P}\tilde{\mathcal{D}}\nu(k)\},\ \mathrm{E}\{\eta^{\mathrm{T}}(k)\mathcal{C}^{\mathrm{T}}\mathcal{P}\mathcal{D}\nu(k)\}=\mathrm{E}\{\eta^{\mathrm{T}}(k)\tilde{\mathcal{C}}^{\mathrm{T}}\mathcal{P}\tilde{\mathcal{D}}\nu(k)\},\\&\mathrm{E}\{g^{\mathrm{T}}(k)\mathcal{G}^{\mathrm{T}}\mathcal{P}\mathcal{D}\nu(k)\}=\mathrm{E}\{-g^{\mathrm{T}}(k)\tilde{\mathcal{G}}^{\mathrm{T}}\mathcal{P}\tilde{\mathcal{D}}\nu(k)\}.\end{aligned}\tag{29}$$

By the similar statements as in the first part of this proof and selecting the augmented vector $\hat{\xi}(k)=[\eta^{\mathrm{T}}(k)\ \mathcal{F}^{\mathrm{T}}\ g^{\mathrm{T}}(k)\ \nu^{\mathrm{T}}(k)]^{\mathrm{T}}$, Eq. (28) can be rearranged as

$$\mathrm{E}\{\Delta V(k)\}\leqslant\mathrm{E}\{\hat{\xi}^{\mathrm{T}}(k)\tilde{\Lambda}\hat{\xi}(k)|\eta(k)\},\tag{30}$$

where $\tilde{\Lambda}=\hat{\Lambda}+\mathrm{diag}\{-\mathcal{H}^{\mathrm{T}}\mathcal{H},0,0,\gamma^2 I\}$.

Choose an index as

$$J\triangleq\sum_{k=0}^{\infty}\mathrm{E}\left\{\bar{z}^{\mathrm{T}}(k)\bar{z}(k)-\gamma^2\nu^{\mathrm{T}}(k)\nu(k)\right\}.\tag{31}$$

Observing the stochastic stability and zero initial condition, we obtain $\sum_{k=0}^{\infty}\mathrm{E}\{\Delta V(k)\}=0$ and

$$\begin{aligned}J&=\sum_{k=0}^{\infty}\mathrm{E}\{\bar{z}^{\mathrm{T}}(k)\bar{z}(k)-\gamma^2\nu^{\mathrm{T}}(k)\nu(k)+\Delta V(k)\}\\&\leqslant\sum_{k=0}^{\infty}\mathrm{E}\{\eta^{\mathrm{T}}(k)\mathcal{H}^{\mathrm{T}}\mathcal{H}\eta(k)-\gamma^2\nu^{\mathrm{T}}(k)\nu(k)+\hat{\xi}^{\mathrm{T}}(k)\tilde{\Lambda}\hat{\xi}(k)\}\\&=\sum_{k=0}^{\infty}\mathrm{E}\{\hat{\xi}^{\mathrm{T}}(k)\hat{\Lambda}\hat{\xi}(k)\},\end{aligned}\tag{32}$$

where $\hat{\Lambda}$ is shown as (12).

In light of (12), system (11) is exponentially stable in the mean square sense and achieves the specified H_∞ performance in Definition 2. That is, the stochastic BRL has been established. This completes the proof.

Remark 4. The stochastic BRL, i.e., the H_∞ performance analysis result, has been established by the aid of Lyapunov stability theory as well as the stochastic analysis techniques. It can be observed that the coexistence of the event-triggered strategy (7) and stochastic parameters $\mathcal{C}$, $\mathcal{D}$, $\mathcal{G}$ remarkably increases the difficulties of performance analysis for system (11).

3.2 Filter synthesis

In this subsection the distributed H_∞ filter (8) will be designed on the basis of Theorem 1.

It can be observed from $\bar{L}_1$ and $\bar{L}_2$ that $c_{ij}L_{ij}$ ($j\in\mathcal{N}_i$) are coupled with $\sqrt{\beta_{ij}^*}$ and $\bar{\beta}_{ij}$, respectively, where β_{ij}^* and $\bar{\beta}_{ij}$ refer to the variance and expectation of the stochastic process β_{ij}^k. If $\sqrt{\beta_{ij}^*}$ and $\bar{\beta}_{ij}$ are not decoupled from $\bar{L}_1$ and $\bar{L}_2$, then $c_{ij}L_{ij}$ cannot been directly determined by the standard design method based on congruence transformation and the matrix substitution technique.

In order to conveniently compute the gain L_{ij} ($i\in\mathcal{N}, j\in\mathcal{N}_i$), the following useful result is presented.

Lemma 1. For matrices $K_1=[g_{ij}K_{ij}]_{N\times N}$, $K_2=[h_{ij}K_{ij}]_{N\times N}$ where g_{ij},h_{ij} ($i,\ j\in\mathcal{N}$) are known scalars and K_{ij} are parameters to be designed, there exist appropriate matrix $W<0$ and diagonal matrix $Q>0$ satisfying $W+K_1^{\mathrm{T}}QK_1+K_2^{\mathrm{T}}QK_2<0$ if and only if there exist matrices Y and $\mathcal{Q}>0$ satisfying

$$\begin{bmatrix}W & W_1^{\mathrm{T}} & W_2^{\mathrm{T}}\\ * & -\mathcal{Q} & 0\\ * & * & -\mathcal{Q}\end{bmatrix}<0,\tag{33}$$

where $W_1=[(\bar{e}_1YG_1)^{\mathrm{T}}\ (\bar{e}_2YG_2)^{\mathrm{T}}\ \cdots\ (\bar{e}_NYG_N)^{\mathrm{T}}]^{\mathrm{T}}$, $W_2=[(\bar{e}_1YH_1)^{\mathrm{T}}\ (\bar{e}_2YH_2)^{\mathrm{T}}\ \cdots\ (\bar{e}_NYH_N)^{\mathrm{T}}]^{\mathrm{T}}$,

$$\mathcal{Q}=\mathrm{diag}\{\underbrace{Q,\ldots,Q}_{N}\},\quad \bar{e}_i=\mathrm{diag}\{\underbrace{0_{n_y},\ldots,}_{i-1}I_{n_y},\underbrace{\ldots,0_{n_y}}_{N-i}\},$$

$G_i=\mathrm{diag}\{g_{i1},\ldots,g_{iN}\}$, $H_i=\mathrm{diag}\{h_{i1},\ldots,h_{iN}\}$. Moreover, the matrix $K=[K_{ij}]_{N\times N}$ can be computed by $K=Q^{-1}Y$.

Proof. By the definitions of G_i, H_i, and $\bar{e}_i$, the matrices K_1 and K_2 can be decomposed as $K_1 = \sum_{i=1}^{N} \bar{e}_i K G_i$ and $K_2 = \sum_{i=1}^{N} \bar{e}_i K H_i$, respectively. Using Schur complements and setting $QK = Y$ where $K = [K_{ij}]_{N\times N}$, we immediately obtain (33) and $K = Q^{-1}Y$.

Inspired by the disposal of matrix factorization in Lemma 1, we now define

$$\bar{L}_1 = \sum_{i=1}^{N} \bar{e}_i \bar{L} \tilde{\Delta}_i, \quad \bar{L}_2 = \sum_{i=1}^{N} \bar{e}_i \bar{L} \Delta_i, \tag{34}$$

where $\bar{L} = [c_{ij}L_{ij}]_{N\times N}$, $\tilde{\Delta}_i = \mathrm{diag}\{\sqrt{\beta_{i1}^*}, \sqrt{\beta_{i2}^*}, \ldots, \sqrt{\beta_{iN}^*}\}$, $\Delta_i = \mathrm{diag}\{\bar{\beta}_{i1}, \bar{\beta}_{i2}, \ldots, \bar{\beta}_{iN}\}$.

Accordingly, the design scheme of the filter (8) is provided in the following result.

Theorem 2. For a prescribed disturbance attenuation level $\gamma > 0$, if there exist diagonal matrix $\mathcal{P} = \mathrm{diag}\{P_1, \mathcal{P}_2\} = \mathrm{diag}\{P_1, P_2, P_3, \ldots, P_{N+1}\} > 0$, matrices $\mathcal{X}$, $\mathcal{Y}$ and scalars $\varepsilon_1 > 0$, $\varepsilon_2 > 0$ such that the following convex optimization problem is feasible:

$$\begin{bmatrix} \Pi & \tilde{\Phi}^{\mathrm{T}} \\ * & -\tilde{\mathcal{P}}_2 \end{bmatrix} < 0, \tag{35}$$

where $\tilde{\mathcal{P}}_2 = \mathrm{diag}\{I_{5N} \otimes \mathcal{P}_2\}$,

$$\Pi = \begin{bmatrix} \Pi_{11} & 0 & \Pi_{13} & 0 & 0 & A^{\mathrm{T}}P_1B \\ * & \Pi_{22} & 0 & -\frac{\varepsilon_1 I}{2} + \frac{\varepsilon_2 \theta I}{2} & 0 & 0 \\ * & * & P_1 - \varepsilon_2 I & 0 & 0 & P_1 B \\ * & * & * & \Pi_{44} & 0 & 0 \\ * & * & * & * & -I & 0 \\ * & * & * & * & * & \Pi_{66} \end{bmatrix}, \quad \tilde{\Phi}^{\mathrm{T}} = \begin{bmatrix} \mathfrak{L}_1^{\mathrm{T}} & \mathfrak{L}_2^{\mathrm{T}} & \mathfrak{L}_3^{\mathrm{T}} & 0 & 0 \\ 0 & 0 & 0 & \mathfrak{L}_4^{\mathrm{T}} & \mathfrak{L}_5^{\mathrm{T}} \\ 0 & 0 & 0 & 0 & 0 \\ 0 & 0 & 0 & 0 & \bar{\Omega}^{\mathrm{T}} \\ 0 & 0 & 0 & \mathfrak{L}_6^{\mathrm{T}} & \mathfrak{L}_7^{\mathrm{T}} \\ 0 & 0 & 0 & \mathfrak{L}_8^{\mathrm{T}} & \mathfrak{L}_9^{\mathrm{T}} \end{bmatrix}$$

with

$$\begin{aligned} &\Pi_{11} = A^{\mathrm{T}}P_1A - P_1 + \varepsilon_1\rho I + \varepsilon_2\phi I + (\bar{\Gamma}\bar{C})^{\mathrm{T}}\Upsilon(\bar{\Gamma}\bar{C}) + (\Gamma\bar{C})^{\mathrm{T}}\Upsilon(\Gamma\bar{C}) + H^{\mathrm{T}}H, \\ &\Pi_{13} = A^{\mathrm{T}}P_1 - \frac{\varepsilon_1 I}{2} + \frac{\varepsilon_2\theta I}{2}, \quad \Pi_{22} = -\mathcal{P}_2 + \varepsilon_1\rho I + \varepsilon_2\phi I + \bar{H}^{\mathrm{T}}\bar{H}, \\ &\Pi_{44} = (1-N)\mathcal{P}_2 - \varepsilon_2 I, \quad \Pi_{66} = B^{\mathrm{T}}P_1B - \gamma^2 I, \end{aligned}$$

and

$$\mathfrak{L}_1 = \begin{bmatrix} \sqrt{\alpha_1^*}\mathcal{X}e_1C_1 \\ \sqrt{\alpha_2^*}\mathcal{X}e_2C_2 \\ \vdots \\ \sqrt{\alpha_N^*}\mathcal{X}e_NC_N \end{bmatrix}, \ \mathfrak{L}_2 = \begin{bmatrix} \sqrt{\alpha_1^*}\bar{e}_1\mathcal{Y}\tilde{\Delta}_1e_1C_1 \\ \sqrt{\alpha_2^*}\bar{e}_2\mathcal{Y}\tilde{\Delta}_2e_2C_2 \\ \vdots \\ \sqrt{\alpha_N^*}\bar{e}_N\mathcal{Y}\tilde{\Delta}_Ne_NC_N \end{bmatrix}, \ \mathfrak{L}_3 = \begin{bmatrix} \sqrt{\alpha_1^*}\bar{e}_1\mathcal{Y}\Delta_1e_1C_1 \\ \sqrt{\alpha_2^*}\bar{e}_2\mathcal{Y}\Delta_2e_2C_2 \\ \vdots \\ \sqrt{\alpha_N^*}\bar{e}_N\mathcal{Y}\Delta_Ne_NC_N \end{bmatrix},$$

$$\mathfrak{L}_4 = \begin{bmatrix} \bar{e}_1\mathcal{Y}\tilde{\Delta}_1\Gamma\tilde{C} \\ \bar{e}_2\mathcal{Y}\tilde{\Delta}_2\Gamma\tilde{C} \\ \vdots \\ \bar{e}_N\mathcal{Y}\tilde{\Delta}_N\Gamma\tilde{C} \end{bmatrix}, \ \mathfrak{L}_5 = \begin{bmatrix} \mathcal{P}_2(I_N\otimes A) - \mathcal{X}\Gamma\tilde{C} - \bar{e}_1\mathcal{Y}\Delta_1\Gamma\tilde{C} \\ \mathcal{P}_2(I_N\otimes A) - \mathcal{X}\Gamma\tilde{C} - \bar{e}_2\mathcal{Y}\Delta_2\Gamma\tilde{C} \\ \vdots \\ \mathcal{P}_2(I_N\otimes A) - \mathcal{X}\Gamma\tilde{C} - \bar{e}_N\mathcal{Y}\Delta_N\bar{L}\Gamma\tilde{C} \end{bmatrix}, \ \mathfrak{L}_6 = \begin{bmatrix} -\bar{e}_1\mathcal{Y}\tilde{\Delta}_1 \\ -\bar{e}_2\mathcal{Y}\tilde{\Delta}_2 \\ \vdots \\ -\bar{e}_N\mathcal{Y}\tilde{\Delta}_N \end{bmatrix},$$

$$\mathfrak{L}_7 = \begin{bmatrix} \mathcal{X} + \bar{e}_1\mathcal{Y}\Delta_1 \\ \mathcal{X} + \bar{e}_2\mathcal{Y}\Delta_2 \\ \vdots \\ \mathcal{X} + \bar{e}_N\mathcal{Y}\Delta_N \end{bmatrix}, \ \mathfrak{L}_8 = \begin{bmatrix} \bar{e}_1\mathcal{Y}\tilde{\Delta}_1\bar{D} \\ \bar{e}_2\mathcal{Y}\tilde{\Delta}_2\bar{D} \\ \vdots \\ \bar{e}_N\mathcal{Y}\tilde{\Delta}_N\bar{D} \end{bmatrix}, \ \mathfrak{L}_9 = \begin{bmatrix} \mathcal{P}_2\bar{B} - \mathcal{X}\bar{D} - \bar{e}_1\mathcal{Y}\Delta_1\bar{D} \\ \mathcal{P}_2\bar{B} - \mathcal{X}\bar{D} - \bar{e}_2\mathcal{Y}\Delta_2\bar{D} \\ \vdots \\ \mathcal{P}_2\bar{B} - \mathcal{X}\bar{D} - \bar{e}_N\mathcal{Y}\Delta_N\bar{D} \end{bmatrix}, \ \bar{\Omega}^{\mathrm{T}} = [\underbrace{\mathcal{P}_2, \mathcal{P}_2, \ldots, \mathcal{P}_2}_{N}],$$

then Eq. (8) is an event-triggered distributed H_∞ filter of system (1), and $\bar{L}$ and $\hat{L}$ can be given by

$$\hat{L} = \mathrm{diag}\{L_{11}, L_{22}, \ldots, L_{NN}\} = \mathcal{P}_2^{-1}\mathcal{X}, \quad \bar{L} = [c_{ij}L_{ij}]_{N\times N} = \mathcal{P}_2^{-1}\mathcal{Y}. \tag{36}$$

Thus, the filter gains L_{ii} and L_{ij} $(i \in \mathcal{N}, j \in \mathcal{N}_i)$ are obtained from the definitions of $\hat{L}$, $\bar{L}$ in (9).

Proof. By Schur complements, Eq. (12) is equivalently written as

$$\Psi \triangleq \begin{bmatrix} \Pi & \tilde{\Phi}_L^{\mathrm{T}} \\ * & -\tilde{\mathcal{P}}_2^{-1} \end{bmatrix} < 0, \tag{37}$$

where

$$\tilde{\Phi}_L^{\mathrm{T}} = \begin{bmatrix} \mathcal{L}_1^{\mathrm{T}} & \mathcal{L}_2^{\mathrm{T}} & \mathcal{L}_3^{\mathrm{T}} & 0 & 0 \\ 0 & 0 & 0 & \mathcal{L}_4^{\mathrm{T}} & \mathcal{L}_5^{\mathrm{T}} \\ 0 & 0 & 0 & 0 & 0 \\ 0 & 0 & 0 & 0 & \Omega^{\mathrm{T}} \\ 0 & 0 & 0 & \mathcal{L}_6^{\mathrm{T}} & \mathcal{L}_7^{\mathrm{T}} \\ 0 & 0 & 0 & \mathcal{L}_8^{\mathrm{T}} & \mathcal{L}_9^{\mathrm{T}} \end{bmatrix}$$

with

$$\mathcal{L}_1 = \begin{bmatrix} \sqrt{\alpha_1^*}\hat{L}e_1C_1 \\ \sqrt{\alpha_2^*}\hat{L}e_2C_2 \\ \vdots \\ \sqrt{\alpha_N^*}\hat{L}e_NC_N \end{bmatrix},\ \mathcal{L}_2 = \begin{bmatrix} \sqrt{\alpha_1^*}\bar{e}_1\bar{L}\tilde{\Delta}_1e_1C_1 \\ \sqrt{\alpha_2^*}\bar{e}_2\bar{L}\tilde{\Delta}_2e_2C_2 \\ \vdots \\ \sqrt{\alpha_N^*}\bar{e}_N\bar{L}\tilde{\Delta}_Ne_NC_N \end{bmatrix},\ \mathcal{L}_3 = \begin{bmatrix} \sqrt{\alpha_1^*}\bar{e}_1\bar{L}\Delta_1e_1C_1 \\ \sqrt{\alpha_2^*}\bar{e}_2\bar{L}\Delta_2e_2C_2 \\ \vdots \\ \sqrt{\alpha_N^*}\bar{e}_N\bar{L}\Delta_Ne_NC_N \end{bmatrix},$$

$$\mathcal{L}_4 = \begin{bmatrix} \bar{e}_1\bar{L}\tilde{\Delta}_1\Gamma\tilde{C} \\ \bar{e}_2\bar{L}\tilde{\Delta}_2\Gamma\tilde{C} \\ \vdots \\ \bar{e}_N\bar{L}\tilde{\Delta}_N\Gamma\tilde{C} \end{bmatrix},\ \mathcal{L}_5 = \begin{bmatrix} I_N\otimes A - \hat{L}\Gamma\tilde{C} - \bar{e}_1\bar{L}\Delta_1\Gamma\tilde{C} \\ I_N\otimes A - \hat{L}\Gamma\tilde{C} - \bar{e}_2\bar{L}\Delta_2\Gamma\tilde{C} \\ \vdots \\ I_N\otimes A - \hat{L}\Gamma\tilde{C} - \bar{e}_N\bar{L}\Delta_N\bar{L}\Gamma\tilde{C} \end{bmatrix},\ \mathcal{L}_6 = \begin{bmatrix} -\bar{e}_1\bar{L}\tilde{\Delta}_1 \\ -\bar{e}_2\bar{L}\tilde{\Delta}_2 \\ \vdots \\ -\bar{e}_N\bar{L}\tilde{\Delta}_N \end{bmatrix},$$

$$\mathcal{L}_7 = \begin{bmatrix} \hat{L} + \bar{e}_1\bar{L}\Delta_1 \\ \hat{L} + \bar{e}_2\bar{L}\Delta_2 \\ \vdots \\ \hat{L} + \bar{e}_N\bar{L}\Delta_N \end{bmatrix},\ \mathcal{L}_8 = \begin{bmatrix} \bar{e}_1\bar{L}\tilde{\Delta}_1\bar{D} \\ \bar{e}_2\bar{L}\tilde{\Delta}_2\bar{D} \\ \vdots \\ \bar{e}_N\bar{L}\tilde{\Delta}_N\bar{D} \end{bmatrix},\ \mathcal{L}_9 = \begin{bmatrix} \bar{B} - \hat{L}\bar{D} - \bar{e}_1\bar{L}\Delta_1\bar{D} \\ \bar{B} - \hat{L}\bar{D} - \bar{e}_2\bar{L}\Delta_2\bar{D} \\ \vdots \\ \bar{B} - \hat{L}\bar{D} - \bar{e}_N\bar{L}\Delta_N\bar{D} \end{bmatrix},\ \Omega^{\mathrm{T}} = [\underbrace{I, I, \ldots, I}_{N}].$$

Performing the congruence transformation to (37) by $\mathrm{diag}\{I, \tilde{\mathcal{P}}_2\}$ and applying the matrix substitutions $\mathcal{P}_2\hat{L} = \mathcal{X}$ and $\mathcal{P}_2\bar{L} = \mathcal{Y}$, then the inequality (35) can be directly derived.

Therefore, from Lemma 1 the matrices $\hat{L}$, $\bar{L}$ can be calculated from $\hat{L} = \mathcal{P}_2^{-1}\mathcal{X}$, $\bar{L} = \mathcal{P}_2^{-1}\mathcal{Y}$ if the convex optimization problem (35) is solvable, and eventually the gains L_{ij} $(i, j \in \mathcal{N})$ can be readily computed. The proof is finally completed.

Remark 5. If the notations $\bar{L}_1$ and $\bar{L}_2$ display as whole ones as in Subsection 3.1 without adopting the decomposition (34), then $\sqrt{\alpha_i^*}\bar{e}_i\bar{L}\tilde{\Delta}_ie_iC_i$ in $\mathcal{L}_2$ and $\sqrt{\alpha_i^*}\bar{e}_i\bar{L}\Delta_ie_iC_i$ in $\mathcal{L}_3$ are replaced with $\sqrt{\alpha_i^*}\bar{L}_1e_iC_i$ and $\sqrt{\alpha_i^*}\bar{L}_2e_iC_i$ $(i \in \mathcal{N})$, respectively. Because of the variance β_{ij}^* and expectation $\bar{\beta}_{ij}$ included in $\bar{L}_1$ and $\bar{L}_2$, respectively, the value of matrix $\bar{L}$ cannot be uniquely determined by the common matrix substitution technique. Therefore, Lemma 1 and the factorization technique (34) are effective to ensure the uniqueness and feasibility of the gain $\bar{L}$.

Remark 6. Theorem 2 in this paper is of polynomial computational complexity that can be bounded by $O(N^3n_x^2)$, where N and n_x indicate the number of sensor nodes and dimension of state variable x, respectively. In other words, the time complexity of Theorem 2 relies polynomially on both N and n_x.

4 A numerical example

A numerical example is used to illustrate the effectiveness of the method.

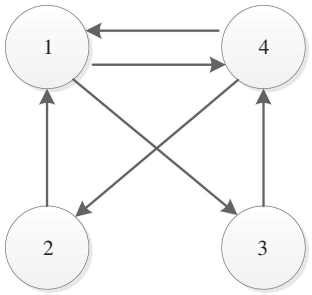

Figure 1 Topology structure of the sensor network.

Example 1. Consider the target plant described by model (1) with four ($N = 4$) sensor nodes and the parameters are given as

$$A = \begin{bmatrix} 0.7 & 0.1 \\ 0.1 & 0.8 \end{bmatrix},\ B = \begin{bmatrix} 0.3 \\ -0.2 \end{bmatrix},\ C_1 = [-0.6\ 0.6],\ C_2 = [-0.5\ 0.8],\ C_3 = [-0.6\ 0.7],\ C_4 = [-0.6\ 0.7],$$
$$D_1 = -0.3,\ D_2 = -0.1,\ D_3 = -0.2,\ D_4 = -0.2,\ H = [-0.4\ 0.4].$$

Select the nonlinear perturbation as $f(k, x(k)) = [-x_1(k)(x_1^2(k) + x_2^2(k)) \ -x_2(k)(x_1^2(k) + x_2^2(k))]^{\mathrm{T}}$. We choose the constants $\rho = 0,\ \theta = -0.2,\ \phi = -0.1$, which clearly satisfy Assumptions 1 and 2. Take the sensor network structure as shown in Figure 1, and the interconnection coefficient c_{ij} is given in the following adjacency matrix:

$$\mathbb{C} = \begin{bmatrix} 1 & \beta_{12}^k \times 0.9 & 0 & \beta_{14}^k \times 0.8 \\ 0 & 1 & 0 & \beta_{24}^k \times 0.8 \\ \beta_{31}^k \times 0.9 & 0 & 1 & 0 \\ \beta_{41}^k \times 0.9 & 0 & \beta_{43}^k \times 0.9 & 1 \end{bmatrix}.$$

The random variables β_{14}^k and β_{41}^k are subject to uniform distributions within the intervals $[0.4, 1.0]$ and $[0.6, 1.0]$, respectively. β_{12}^k, β_{24}^k, β_{31}^k, and β_{43}^k obey the Bernoulli distributions with the first moments 0.65, 0.85, 0.85, 0.85, respectively. And, $\beta_{ii}^k = 1$ $(i = 1, 2, 3, 4)$, which means that they are time-invariant.

Assume the probabilistic characteristic of measurement $\alpha_i(k)$ is described by Bernoulli distributed random variables with $\bar{\alpha}_1 = 0.85$, $\bar{\alpha}_2 = 0.80$, $\bar{\alpha}_3 = 0.90$, $\bar{\alpha}_4 = 0.80$. The thresholds of the event-triggered condition in (4) are selected as $\sigma_1 = 0.2$, $\sigma_2 = 0.3$, $\sigma_3 = 0.4$, $\sigma_4 = 0.3$.

By setting $\gamma = 0.8$, the following filter gains can be obtained by solving Theorem 2:

$$L_{11} = \begin{bmatrix} -0.1604 \\ 0.1516 \end{bmatrix},\ L_{12} = \begin{bmatrix} -0.0028 \\ 0.0017 \end{bmatrix},\ L_{14} = \begin{bmatrix} -0.0050 \\ 0.0031 \end{bmatrix},\ L_{22} = \begin{bmatrix} -0.0740 \\ 0.1425 \end{bmatrix},\ L_{24} = \begin{bmatrix} -0.0053 \\ 0.0033 \end{bmatrix},$$
$$L_{31} = \begin{bmatrix} -0.0051 \\ 0.0032 \end{bmatrix},\ L_{33} = \begin{bmatrix} -0.1244 \\ 0.1495 \end{bmatrix},\ L_{41} = \begin{bmatrix} -0.0052 \\ 0.0032 \end{bmatrix},\ L_{43} = \begin{bmatrix} -0.0032 \\ 0.0020 \end{bmatrix},\ L_{44} = \begin{bmatrix} -0.1117 \\ 0.1495 \end{bmatrix}.$$

The exogenous noise is chosen as $\nu(k) = 1/k^2$. The initial conditions are $x(0) = [-0.5\ 0.4]^{\mathrm{T}}$ and $\hat{x}_1(0) = [-0.8\ 0.9]^{\mathrm{T}}$, $\hat{x}_2(0) = [-0.9\ 0.7]^{\mathrm{T}}$, $\hat{x}_3(0) = [-0.3\ -0.1]^{\mathrm{T}}$, $\hat{x}_4(0) = [-0.7\ 0.9]^{\mathrm{T}}$. Figure 2 shows the event triggering time instants of each sensor node. It is evident that only partial measurement signals will be transmitted to the filters via the common communication channels. Thus, the event-triggered transmission strategy is indeed efficient to mitigate the communication burden. The states and their corresponding estimates are shown in Figures 3 and 4, respectively. Figure 5 depicts the output estimation errors. Apparently, the satisfactory performance can be achieved under the constructed event-triggered filter (8).

5 Conclusion

This paper proposed an event-based distributed H_∞ filter design for one-sided Lipschitz nonlinear systems with fading measurements over a sensor network with a randomly varying topology. The one-sided

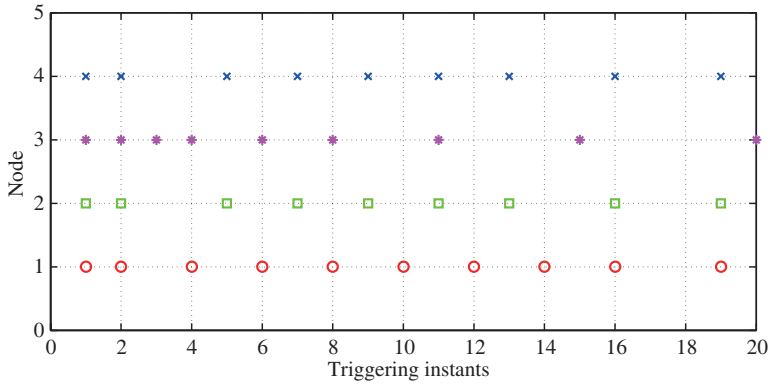

Figure 2 (Color online) Event triggering instants.

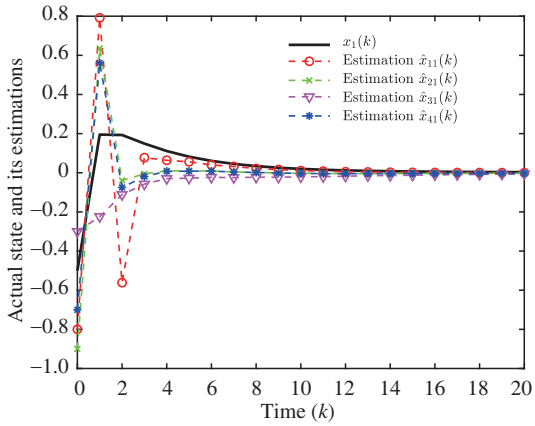

Figure 3 (Color online) $x_1(k)$ and its estimation.

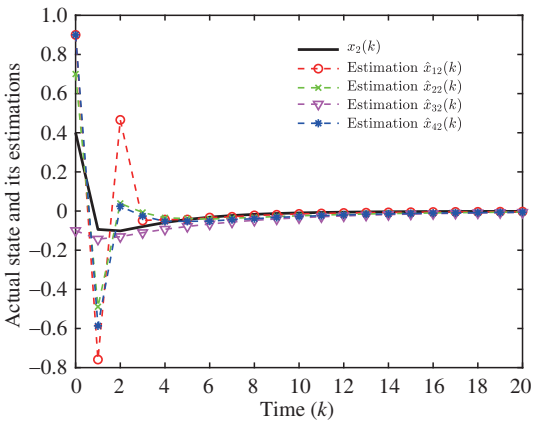

Figure 4 (Color online) $x_2(k)$ and its estimation.

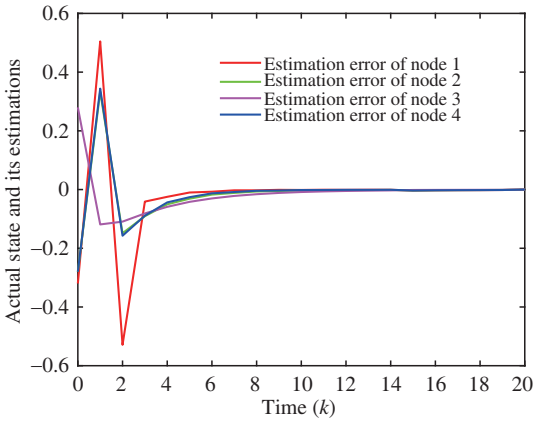

Figure 5 (Color online) Output estimation error.

Lipschitz condition is a generalized form of the conventional Lipschitz constraint. The randomness of the interconnection coefficient between any pair of adjacent sensor nodes was described by a random variable with a known probabilistic distribution. The data transmission was scheduled by an event-based policy. Moreover, the stochastic BRL was obtained, and the desired event-triggered distributed H_∞ filter was effectively designed using the matrix decomposition method. In the near future, we will extend our theoretical approach to practical applications, especially, to distributed recursive filtering [8, 29] and distributed set-membership filtering [25] under communication protocols [18, 20–22, 48] over sensor networks with random topologies (5).

Acknowledgements This work was supported partially by Zhejiang Provincial Natural Science Foundation (Grant No. LR16F0-

30003) and partially by National Natural Science Foundation of China (Grant Nos. 61973102, U1509205).

References

1 Shuman D I, Nayyar A, Mahajan A, et al. Measurement scheduling for soil moisture sensing: from physical models to optimal control. Proc IEEE, 2010, 98: 1918–1933
2 Lamont L, Toulgoat M, Déziel M, et al. Tiered wireless sensor network architecture for military surveillance applications. In: Proceedings of the 5th International Conference on Sensor Technologies and Applications, Nice, 2011. 288–295
3 Ezdiani S, Acharyya I S, Sivakumar S, et al. Wireless sensor network softwarization: towards WSN adaptive QoS. IEEE Int Things J, 2017, 4: 1517–1527
4 Ge X, Han Q L, Zhang X M, et al. Distributed event-triggered estimation over sensor networks: a survey. IEEE Trans Cybern, 2020, 50: 1306–1320
5 Chen Y, Chen Z P, Chen Z Y, et al. Observer-based passive control of non-homogeneous Markov jump systems with random communication delays. Int J Syst Sci, 2020, 51: 1133–1147
6 Olfati-Saber R. Distributed Kalman filtering for sensor networks. In: Proceedings of the 46th IEEE Conference on Decision and Control, New Orleans, 2008. 5492–5498
7 Zhang D, Cai W J, Xie L H, et al. Nonfragile distributed filtering for T-S fuzzy systems in sensor networks. IEEE Trans Fuzzy Syst, 2015, 23: 1883–1890
8 Ding D, Wang Z, Ho D W C, et al. Distributed recursive filtering for stochastic systems under uniform quantizations and deception attacks through sensor networks. Automatica, 2017, 78: 231–240
9 Ma L F, Wang Z D, Lam H K, et al. Distributed event-based set-membership filtering for a class of nonlinear systems with sensor saturations over sensor networks. IEEE Trans Cybern, 2017, 47: 3772–3783
10 Alyazidi N M, Mahmoud M S. Distributed H_2/H_∞ filter design for discrete-time switched systems. IEEE/CAA J Autom Sin, 2020, 7: 158–168
11 Chen Y, Wang Z D, Yuan Y, et al. Distributed H_∞ filtering for switched stochastic delayed systems over sensor networks with fading measurements. IEEE Trans Cybern, 2020, 50: 2–14
12 Zhang L X, Gao H J, Kaynak O. Network-induced constraints in networked control systems — a survey. IEEE Trans Ind Inf, 2013, 9: 403–416
13 Liang J L, Wang Z D, Liu X H. Distributed state estimation for discrete-time sensor networks with randomly varying nonlinearities and missing measurements. IEEE Trans Neural Netw, 2011, 22: 486–496
14 Wang D, Wang Z D, Li G Y, et al. Distributed filtering for switched nonlinear positive systems with missing measurements over sensor networks. IEEE Sens J, 2016, 16: 4940–4948
15 Li W L, Jia Y M, Du J P. Distributed filtering for discrete-time linear systems with fading measurements and time-correlated noise. Digit Signal Process, 2017, 60: 211–219
16 Chen Y, Chen C, Xue A. Distributed non-fragile $l_2 - l_\infty$ filtering over sensor networks with random gain variations and fading measurements. Neurocomputing, 2019, 338: 154–162
17 Oki E, Jing Z G, Rojas-Cessa R, et al. Concurrent round-robin-based dispatching schemes for Clos-network switches. IEEE/ACM Trans Netw, 2002, 10: 830–844
18 Xu Y, Lu R Q, Shi P, et al. Finite-time distributed state estimation over sensor networks with round-robin protocol and fading channels. IEEE Trans Cybern, 2018, 48: 336–345
19 Li J Y, Zhang B, Lu R Q, et al. Distributed H_∞ state estimator design for time-delay periodic systems over scheduling sensor networks. IEEE Trans Cybern, 2021, 51: 462–472
20 Zou L, Wang Z D, Gao H J, et al. Finite-horizon $\mathcal{H}_\infty$ consensus control of time-varying multiagent systems with stochastic communication protocol. IEEE Trans Cybern, 2017, 47: 1830–1840
21 Wang J H, Song Y. Resilient RMPC for cyber-physical systems with polytopic uncertainties and state saturation under TOD scheduling: an ADT approach. IEEE Trans Ind Inf, 2020, 16: 4900–4908
22 Zhao Y, He X, Zhou D H. Distributed filtering for time-varying networked systems with sensor gain degradation and energy constraint: a centralized finite-time communication protocol scheme. Sci China Inf Sci, 2018, 61: 092208
23 Tabuada P. Event-triggered real-time scheduling of stabilizing control tasks. IEEE Trans Autom Control, 2007, 52: 1680–1685
24 Ma H, Li H Y, Lu R Q, et al. Adaptive event-triggered control for a class of nonlinear systems with periodic disturbances. Sci China Inf Sci, 2020, 63: 150212
25 Ma L F, Wang Z D, Han Q L, et al. Consensus control of stochastic multi-agent systems: a survey. Sci China Inf Sci, 2017, 60: 120201
26 Xia J W, Li B M, Su S F, et al. Finite-time command filtered event-triggered adaptive fuzzy tracking control for stochastic nonlinear systems. IEEE Trans Fuzzy Syst, 2021, 29: 1815–1825
27 Yue D, Tian E, Han Q L. A delay system method for designing event-triggered controllers of networked control systems. IEEE Trans Autom Control, 2013, 58: 475–481
28 Xia W F, Zheng W X, Xu S Y. Event-triggered filter design for Markovian jump delay systems with nonlinear perturbation using quantized measurement. Int J Robust Nonlinear Control, 2019, 29: 4644–4664
29 Liu Q Y, Wang Z D, He X, et al. Event-based recursive distributed filtering over wireless sensor networks. IEEE Trans Autom Control, 2015, 60: 2470–2475
30 Su H S, Wang X, Zeng Z G. Consensus of second-order hybrid multiagent systems by event-triggered strategy. IEEE Trans Cybern, 2020, 50: 4648–4657
31 Xu W Y, Ho D W C, Zhong J, et al. Event/self-triggered control for leader-following consensus over unreliable network with DoS attacks. IEEE Trans Neural Netw Learn Syst, 2019, 30: 3137–3149
32 Hu J, Liu G P, Zhang H, et al. On state estimation for nonlinear dynamical networks with random sensor delays and coupling strength under event-based communication mechanism. Inf Sci, 2020, 511: 265–283
33 Khalil H K. Nonlinear Systems. 3rd ed. Englewood Cliffs: Prentice Hall, 2002
34 Abbaszadeh M, Marquez H J. Nonlinear observer design for one-sided Lipschitz systems. In: Proceedings of American Control Conference, Baltimore, 2010. 5284–5289
35 Song J, He S P. Robust finite-time H_∞ control for one-sided Lipschitz nonlinear systems via state feedback and output feedback. J Franklin Inst, 2015, 352: 3250–3266
36 Agha R, Rehan M, Ahn C K, et al. Adaptive distributed consensus control of one-sided Lipschitz nonlinear multiagents. IEEE Trans Syst Man Cybern Syst, 2019, 49: 568–578
37 Yang W, Zhang Y, Chen G R, et al. Distributed filtering under false data injection attacks. Automatica, 2019, 102: 34–44

38 Shen B, Wang Z D, Ding D R, et al. H_∞ state estimation for complex networks with uncertain inner coupling and incomplete measurements. IEEE Trans Neural Netw Learn Syst, 2013, 24: 2027–2037

39 You K Y, Li Z K, Xie L H. Consensus condition for linear multi-agent systems over randomly switching topologies. Automatica, 2013, 49: 3125–3132

40 Ugrinovskii V. Distributed robust estimation over randomly switching networks using H_∞ consensus. Automatica, 2013, 49: 160–168

41 Yan H C, Yang Q, Zhang H, et al. Distributed H_∞ state estimation for a class of filtering networks with time-varying switching topologies and packet losses. IEEE Trans Syst Man Cybern Syst, 2018, 48: 2047–2057

42 Zhang Q, Zhang J F. Distributed parameter estimation over unreliable networks with Markovian switching topologies. IEEE Trans Autom Control, 2012, 57: 2545–2560

43 Liu Q Y, Wang Z D, He X, et al. Event-based distributed filtering over Markovian switching topologies. IEEE Trans Autom Control, 2019, 64: 1595–1602

44 He M H, Mu J R, Mu X W. H_∞ leader-following consensus of nonlinear multi-agent systems under semi-Markovian switching topologies with partially unknown transition rates. Inf Sci, 2020, 513: 168–179

45 Ma L F, Wang Z D, Liu Y R, et al. Distributed filtering for nonlinear time-delay systems over sensor networks subject to multiplicative link noises and switching topology. Int J Robust Nonlinear Control, 2019, 29: 2941–2959

46 Li W L, Jia Y M, Du J P. State estimation for stochastic complex networks with switching topology. IEEE Trans Autom Control, 2017, 62: 6377–6384

47 Bioucas-Dias J M, Figueiredo M A T. Multiplicative noise removal using variable splitting and constrained optimization. IEEE Trans Image Process, 2010, 19: 1720–1730

48 Chen Y, Wang Z D, Wang L C, et al. Finite-horizon H_∞ state estimation for stochastic coupled networks with random inner couplings using round-robin protocol. IEEE Trans Cybern, 2021, 51: 1204–1215